Calcium transients induce spatially coordinated increases in traction force during the movement of fish keratocytes

Andrew Doyle[1], William Marganski[2] and Juliet Lee[1,*]

[1]Department of Molecular and Cell Biology, University of Connecticut, Storrs, CT 06269, USA
[2]Department of Biomedical Engineering, Boston University, Boston, MA 02215, USA
*Author for correspondence (e-mail: jlee@uconnvm.uconn.edu)

Accepted 7 January 2004
Journal of Cell Science 117, 2203-2214 Published by The Company of Biologists 2004
doi:10.1242/jcs.01087

Summary

The coordination of protrusion with retraction is essential for continuous cell movement. In fish keratocytes the activation of stretch-activated calcium channels, and the resulting increase in intracellular calcium, trigger release of the rear cell margin when forward movement is impeded. Although it is likely that retraction involves a calcium-dependent increase in cytoskeletal contractility, it is not known how the timing, magnitude and localization of contractile forces are organized during retraction. We have addressed this question using a new gelatin traction force assay in combination with calcium imaging to determine what changes in cytoskeletal force production accompany calcium-induced retraction. We find that individual calcium transients are followed within seconds by a rapid increase in traction stress that is maintained, or increases in a stepwise manner, until retraction occurs. Increases in traction stress are accompanied by a distinct sequence of changes in the spatial distribution of large traction stresses. Regions of increased traction stress enlarge at the lateral cell margins and expand forward along the cell margin. In particular, rearward facing propulsive' tractions at the leading edge of the cell, which are normally very low, increase several fold. Following retraction, a precipitous drop in traction stress is observed. Such distinct variations in traction stress are not observed in cells when calcium transients are absent. These results suggest a mechanism by which global increases in intracellular calcium can locally regulate contractile force production, in order to maintain a rapid highly directed mode of movement.

Key words: Calcium transients, Traction force, Keratocyte, Movement

Introduction

Cell movement is dependent on the spatial and temporal organization of cytoskeletal function such that new adhesions and protrusion occur at the front of the cell while detachment of adhesions and retraction occur at the rear (Mitchison and Cramer, 1996; Pollard and Borisy, 2003). Although much has been learnt about the molecular mechanisms involved in each of these processes, little is known about how they are coordinated with each other. However, a growing number of studies indicate that cytoskeletal force generation is involved in coordinating different cytoskeletal functions (Lauffenburger and Horwitz, 1996). For example, increased cytoskeletal tension promotes retraction but inhibits protrusion (Kolega, 1986). Conversely, decreased contractility favors protrusion (Lee et al., 1994; Oliver et al., 1999). In addition, integrin containing adhesions can be strengthened by increases in cytoskeletal force production (Chrzanowska-Wodnicka and Burridge, 1996; Choquet et al., 1997; Riveline et al., 2001) but are weakened when this is reduced (Oliver et al., 1999). Thus the magnitude, timing and location of contractile force generation must be tightly regulated, so that alternate cycles of protrusion and retraction can occur. However, it is not known how the temporal and spatial organization of contractility is regulated.

The development of a variety of traction force assays has provided much insight into how cytoskeletal contractile forces are utilized in movement (Wang and Pelham, 1998; Galbraith and Sheetz, 1997a; Burton et al., 1999; Doyle and Lee, 2002; Tan et al., 2003). These generally consist of a flexible surface that can be deformed in response to the contractile forces that a moving cell exerts on them. The deformations are then used to draw more or less precise inferences about the magnitude, direction and location of the traction forces that moving cells exert upon their substrata. In general, the magnitude and spatial distribution of traction forces is related to cell shape and mode of movement (Galbraith and Sheetz, 1997b; Oliver et al., 1999). For example, normal 3T3 fibroblasts are relatively large cells (area ~2000 μm^2) that move at a speed of ~0.5 μm/minute. The traction pattern during fibroblast movement is characterized by large rearward directed (propulsive) tractions concentrated in a narrow band behind the leading edge and forward directed (frictional) tractions concentrated at the trailing edge where detachment occurs (Dembo and Wang, 1999). The area-average of the traction magnitude in 3T3 fibroblasts is ~20 kdynes/cm^2. By contrast, fish keratocytes have about 20% of the area of fibroblasts and can move very rapidly (~30 microns/minute) while maintaining a characteristic 'fan' shape. The area average of the traction magnitude in keratocytes (~2 kdynes/cm^2) is significantly smaller than the value in fibroblasts, but more

importantly the qualitative pattern of traction forces is quite different. In particular, the largest traction forces (the so-called 'pinching' tractions) are located at the lateral cell edges (or 'wings') and oriented perpendicular to the direction of cell motion. It has been suggested that this organization of traction forces permits a rapid rate of protrusion at the leading cell edge, while simultaneously promoting retraction at the rear (Lee et al., 1994). Interestingly, under certain conditions the trailing edge of a keratocyte can fail to detach, in which case the cell gets stuck and forward motion drops dramatically. When this happens, the cell develops a shape and traction pattern that resembles fibroblasts (Oliver et al., 1999). This emphasizes the importance of orchestrated changes in the magnitude and distribution of traction forces in response to the environmental cues and raises the question how this is achieved by moving cells.

Intracellular calcium has long been implicated in the regulation of myosin II-dependent cytoskeletal contractility (Citi and Kendrick-Jones, 1987; Rees et al., 1989; Kamm and Stull, 2000; Chew et al., 2001). In addition the movement of highly motile cell types has been shown to be dependent on transient increases in intracellular calcium (Marks and Maxfield, 1990; Nebl and Fisher, 1997) or a sustained increase in $[Ca^{2+}]_i$ at the rear (Brundage et al., 1991; Gilbert et al., 1994). Increased intracellular calcium facilitates retraction of the rear cell margin by inducing the disassembly of cell-substratum adhesions (Hendey et al., 1992; Huttenlocher et al., 1997; Giannone et al., 2002), increasing cytoskeletal contractility (Walker et al., 1998; Eddy et al., 2000; Zeng et al., 2000) or possibly a combination of both (Crowley and Horwitz, 1995; Palecek et al., 1998). The activation of calcium sensitive actin binding proteins such as gelsolin, has also been implicated in retraction (Hartwig and Yin, 1988).

Increases in intracellular calcium normally occur in response to environmental signals such as chemoattractants (Cheek, 1989). However, in keratocytes calcium transients are triggered by the activation of stretch-activated calcium channels (SAC's), in response to increases in cytoskeletal tension that occur when cell movement is temporarily impeded (Lee et al., 1999). Calcium transients involve global increases in $[Ca^{2+}]_i$ that range from ~219-683 nM, from a baseline value of ~138 nM, as determined from ratiometric measurements (Lee et al., 1999). Shortly after a SAC-mediated calcium transient, retraction occurs allowing cell movement to continue.Thus SACs provide a positive feedback mechanism that promotes a rapid mode of movement.

The findings described above have led us to hypothesize that calcium may regulate the timing and possibly the location of contractile force generation. To test this idea, we have measured the spatio-temporal changes in traction stress, that accompany calcium transients in moving keratocytes. To do this we have used a new gelatin based traction force assay in combination with high resolution calcium imaging (Doyle and Lee, 2002). We have found that single calcium transients can upregulate traction stress, until retraction occurs, which then leads to a precipitous drop in traction stress. During increases in traction stress, an enlargement of regions producing the highest traction stress occurs that begins at the lateral cell edges and spreads forward along the cell margin to the leading edge. Based on these observations, we propose a model to explain how global increases in $[Ca^{2+}]_i$ lead to local changes in contractile force generation and why this may be important for maintaining a rapid, highly directed mode of movement.

Materials and Methods

Preparation and calibration of the gelatin substrata

Gelatin substrata were prepared as described previously (Doyle et al., 2002). Briefly, stock gels were made with 2.5 or 3.0% gelatin (Nabisco, Parsippany, NJ) dissolved in pre-warmed (~40°C) Ca^{2+} and Mg^{2+} free Fish Ringer's solution. Stock gels were liquefied at 40°C and 400 μl was transferred into a Rapport chamber. The gelatin was allowed to solidify at 4°C prior to addition of a solution containing either Flash Red (Bangs Laboratories, Fishers, USA) or blue fluorescent microspheres (0.2 μm, 1:100 in distilled water, Molecular Probes), which was aspirated off immediately. The remaining bead solution was allowed to dry on to the gelatin substratum for one hour at 4°C under airflow. Gelatin substrata were briefly (5-15 seconds) warmed on a hot plate to liquefy the lower layer of gelatin. After removal from the hot plate, ~330 μl of the gelatin solution was carefully removed from the bottom of the chamber using a small pipette tip, being careful not to disturb the surface. Gels were then rapidly cooled for 30 seconds by placing cell chambers on a level metal sheet, pre-cooled to –20°C. This produced a thin layer of gelatin (~40 μm in thickness) whose top surface was embedded with a monolayer of fluorescent beads.

Calibrations of the substrata were performed by placing a steel ball (diameter 0.3-0.4 mm, density 14.95 g/cm^3, Hoover Precision, East Gramby, CT, USA) on the substratum and measuring the resulting surface indentation (Lo et al., 2000). Since gelatin is very hydrophilic the combination of polymer and water is almost incompressible and the Poisson's ratio (ν) is taken to be 0.5. The Young's Modulus (E) is given by $E=3(1-\nu^2)f/(4d^{3/2}r^{1/2})$, where r is the bead radius, f is the force of gravity acting on the steel ball, and d is the depth of the resulting indentation (Radmacher et al., 1992). For the substrates used in this study, E was approximately 2 kPa with a range of ±10%. Substrates were also found to be spatially homogeneous, with measurements of E at different random locations showing about 10% variation from the mean. Finally, we could not detect any hysteresis in the gelatin substrata. Thus beads that were displaced by microneedle manipulation returned to their original positions within less than a second after the needle was removed.

Preparation of cells for calcium imaging

Fish epithelial keratocytes were cultured from Molly fish *Poecillia sphenops* scales as described previously (Lee et al., 1993). Keratocytes were loaded with the calcium indicator Calcium Green-1-dextran (3 kDa, Molecular Probes, Eugene, OR) and the calcium insensitive dye Texas Red-dextran (3 kDa) using the Influx pinocytic cell-loading reagent (Molecular Probes), which was modified for use with keratocytes, before being replated onto gelatin substrata (Fig. 1) (Doyle et al., 2002).

Calcium imaging

Except where noted, calcium imaging was performed as described previously (Ishihara et al., 1997). Prior to imaging, culture medium was replaced with L-15 medium supplemented with ~2% serum, without antibiotics or antifungal agents, to reduce background fluorescence. Calcium imaging was performed on an inverted microscope (Eclipse TE 300; Nikon, Melville, NY) using a Plan APO 100X, 1.4 NA oil emersion objective (Nikon). Fluorescence excitation was achieved using a Ludl high-speed dual filter wheel (Ludl electronic products, Hawthorne, NY) equipped with HQ500/20 and D560/40 excitation filters as well as 10% and/or 32% neutral density filters (Chroma Technology, Brattleboro, VT) for visualization of

Calcium Green-1-dextran and the marker beads. Emission spectra were obtained with a DAPI/FITC/Texas Red triple band pass filter set (Chroma Technology). Cells were exposed for 0.3 and 0.16 seconds to the HQ500/20 and D560/40 excitation spectra, respectively. Images were acquired using a back-illuminated, back thinned, frame transfer CCD camera (Quantix 57, Roper Scientific, Tucson, AZ). Isee Analytical Imaging Software (Isee Imaging Systems, Raleigh, NC) running on a Unix computer platform (SGI O^2, Silicon Graphics, Mountain View, CA) controlled both the camera and filter wheel. Images of Calcium Green-1 loaded keratocytes and marker beads were collected approximately every 1.8 seconds, for several minutes and stored on the computer hard drive (Fig. 1A,B). Triple imaging of some cells was performed on a Zeiss Axiovert 200M inverted microscope (Carl Zeiss MicroImaging, Thornwood, NY) using a Zeiss 100X, 1.4 N.A. emersion oil objective and which was equipped with a DG-4 filter-changer (Sutter Instruments, Novato, CA). Galvometer settings on the DG-4 were adjusted to optimize the excitation of each fluorophore. Cells were exposed for 0.3, 0.15, and 0.1 seconds to the FITC, Texas Red, and Cy-5/DAPI excitation spectra respectively, every ~1.8 seconds. A DAPI/FITC/Texas Red/Cy-5 quad band pass filter set (Chroma Technology) was used for emission spectra. The filter changer and an Orca II CCD camera (Hamamatsu, Bridgewater, NJ) were controlled by Openlab software (Improvision) running on an Apple Macintosh G4 computer. To detect changes in $[Ca^{2+}]_i$, the average fluorescence intensity was measured over the cell body region in sequential images. The background fluorescence was then subtracted from these measurements to correct for any variations in intensity of the light source (100W mercury arc lamp).

Measurement of substrate displacement

For each period of observation a series of images is obtained of beads in their displaced (or disturbed) positions (Fig. 1B) and one reference image of beads in their undisplaced positions, after the cell has moved away. Superimposition of the disturbed bead image onto a reference bead image (Fig. 1C) shows the size and direction of bead displacements. Displacement of the substratum is calculated by comparing the positions of marker beads between the disturbed and reference image, using a correlation-based optical flow algorithm (Marganski et al., 2003). This program determines substratum deformation by finding the best match in the pattern of fluorescent intensity between a small square sub-region of the reference image, and a similar region in the disturbed image. Generally, the sub-regions (also called correlation boxes) are 11 pixels on a side, and the motion is determined for sub-regions centered at 1024 locations in a square grid covering the entire optical field. Typically the maximum magnitude of substrate displacement by a keratocyte is about 4 μm with average displacement of the substrate being about 10-fold smaller. The individual measurements of displacement by this method are generally accurate to about ±0.2 of a pixel (±0.05 μm).

Generation of traction maps

Using the traced cell outline as a guide, a custom algorithm is then used to generate a mesh of approximately 200 quadrilateral elements tessellating the interior of the cell. The most likely traction vector at each node of this mesh is then estimated by fitting the displacement data using the formulas of Boussinesque, that relate substrate displacement to delta function forces acting at the substrate surface. Since a cell cannot apply a net force or torque on the substrate the fitting routine also includes elements that enforce these necessary constraints (Dembo and Wang, 1998).

Results

General character of the keratocyte traction field on gelatin substrata

The shape and movement of keratocytes on gelatin substrata is similar to what has been observed previously on cross-linked silicone or glass surfaces (Lee et al., 1994; Oliver et al., 1999). Fig. 2A shows the outline of a moving fish keratocyte, traced from an image of the cell loaded with a calcium-insensitive, Texas Red-conjugated dextran. Arrows represent the associated pattern of bead displacements in the surrounding gelatin. The head of each arrow corresponds to the position of a material particle of the substrate when the cell is present and the base corresponds to the location of this same particle after the cell has moved far away. The observed pattern of substratum displacements is similar to what was seen previously using cross-linked silicone substrata. The largest bead displacements are found facing inward with respect to the lateral cell margins and smaller inward facing bead displacements are seen at the front lateral cell edges. However, in contrast to previous studies

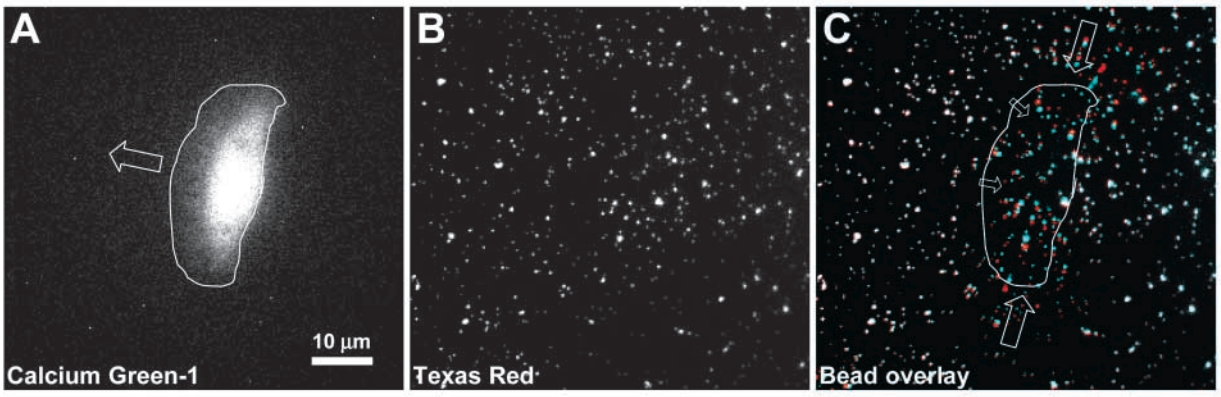

Fig. 1. Dual calcium and traction force imaging in a keratocyte moving on a gelatin substratum. (A) Fluorescence image of a fish keratocyte (white outline) loaded with the calcium indicator, Calcium Green-1-dextran moving in the direction indicated (open arrow). (B) Image of fluorescent beads (0.19-0.20 μm diameter) in their displaced positions within a 3.0% gelatin substratum, upon which the keratocyte in A is moving. (C) Image of fluorescent beads in their undisplaced positions (red) superimposed on panel B (blue beads) and the cell outline in panel A. Comparison of red and blue bead images represents the size and direction of bead displacements caused by the cell in its current position. Beads that do not undergo displacement appear white. The largest bead displacements occur perpendicular to the lateral cell edges (large open arrows) while smaller displacements can be seen within the leading lamella in the direction indicated (small open arrows).

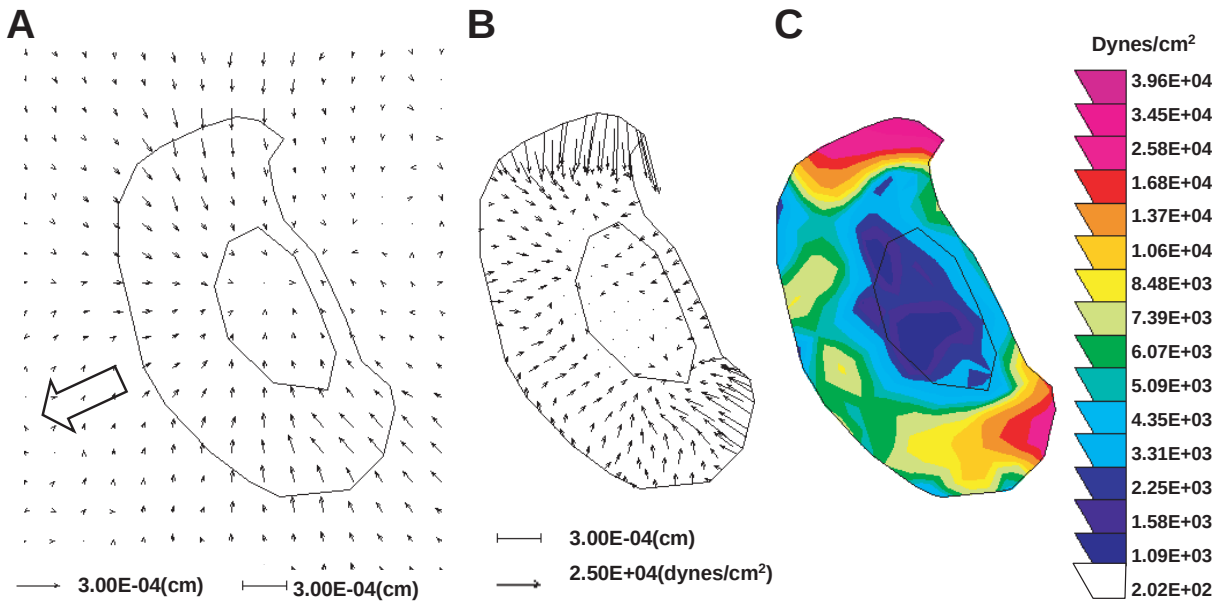

Fig. 2. Generation of traction vector maps using the gelatin traction force assay. (A) A vector map of the experimental bead displacements generated by the optical flow algorithm (Marganski and Dembo, 2003) with an outline of the cell edge and cell body superimposed upon it. The direction and size of the vectors indicate the direction and magnitude of bead displacements occurring in the plane of the substratum, generated by a moving keratocyte. (B) A vector map of traction stress computed from the bead displacements in panel A. Arrows indicate the size and direction of traction stresses. (C) A contour map showing areas of similar traction magnitude. Regions of low and high traction stress are represented by cool (blue-light green) and warm (yellow-purple) colors, respectively.

we observe small rearward directed bead displacements at the leading edge and beneath the remainder of the lamella. One reason we are able to detect these forces is because the spatial resolution of gelatin substrata is about an order of magnitude greater than for silicone substrata. This is due to the fact that substrate deformations can be automatically determined, with sub-pixel accuracy, at thousands of locations in and around the cell periphery, using the optical flow algorithm (Marganski et al., 2003). In addition, the 'stress contrast' of the gelatin traction force assay is higher than for silicone substrata. This means that large traction stresses will not 'overshadow' smaller ones, even if they are close together. Thus the low stress contrast of silicone substrata makes the detection of traction stresses at the leading edge unlikely because the large lateral traction forces will obscure detection of smaller ones elsewhere.

The calculated traction field based on the cell outline and the measured displacements, observed in Fig. 2A are shown in Fig. 2B,C. In Fig. 2B the tractions are represented by arrows that show direction and magnitude of the traction stress acting at each vertex of a pre-specified mesh that fills the cell boundary. Sites where the traction vector is statistically significant are indicated by a small dot. In Fig. 2C we represent the same field using a color contour plot to show regions of similar traction magnitude. The main features of these images are the regions of intense transverse or 'pinching' tractions at the lateral cell edges. The maximum traction force generated by this cell is about 40 kdynes/cm^2, and the average traction magnitude is ~6 kdynes/cm^2 which is about five times higher than the values obtained in previous studies of keratocytes moving on silicone. However, this value is very similar to the traction magnitudes previously detected in 3T3 fibroblasts (Dembo and Wang, 1999). This is somewhat surprising in light of the very different size and behavior of these two cell types. However, this may be related to the fact that keratocytes attach and spread on gelatin surfaces more readily than on cross-linked silicone (J.L., unpublished). Another difference between these traction maps and those obtained from silicone substrata, is the presence of small inward facing 'propulsive' tractions beneath front portions of the lamella (Fig. 2B). In addition small 'frictional' tractions are seen along the back cell edge, while the smallest traction forces are seen beneath the cell body.

Calcium transients lead to an increase in traction force production

To determine whether calcium transients lead to increases in cytoskeletal contractility, we performed dual calcium and traction force imaging of keratocytes moving on gelatin substrata. As reported previously, the frequency at which calcium transients are observed during any given period of observation can vary from zero to more than six (Lee et al., 1999). Here we examined 11 cells that displayed one or more distinct transients, giving a total of 23 calcium transients (Table 1).

To quantify the increases in traction force following a single calcium transient, a series of traction maps were made for each time point (Fig. 3) and compared with double plots of calcium indicator fluorescence and 90th percentile (which we define as being high) traction stress (Fig. 3E). In 21 out of 23 cases calcium transients were followed by an increase in traction force. In this example, an increase in the 90th percentile traction stress is seen almost immediately after the rise in calcium and continues to increase, reaching a maximum of ~11

Table 1. Changes in traction stress associated with single calcium transients

Cell no.	Transient no.	Pre-transient t.s. (dynes/cm^2)	Max t.s. (dynes/cm^2)	Post-transient t.s. (dynes/cm^2)	% increase (all transients)	% change (no retraction)	% change (retraction)
1	1	3130	4860	2270	55		–27
	2	2410	2100	1550	*–23	*–36	
	3	969	918	367	*–5	*–64	
	4	542	1590	1150	193	112	
2	1	5800	10,400	8720	79		50
	2	8720	12,700	12,400	46	42	
	3	12,400	14,000	13,800	13	11	
	4	13,800	15,200	10,000	10		–28
3	1	15,200	27,700	14,000	82		–8
	2	15,900	26,100	23,200	64	46	
4	1	20,000	27,100	16200	36		–19
5	1	5051	5310	2710	5		–46
	2	2000	5910	5730	196	187	
	3	5940	7470	7080	26	19	
	4	6760	8730	8730	29	29	
6	1	6540	11000	8280	68	27	
7	1	12,000	13,800	11,800	15	–2	
8	1	41,400	45,900	36,400	11		–12
9	1	8280	9080	6030	10		–27
10	1	11,500	14,200	12,400	23		8
	2	12,400	16,500	14,800	33	19	
	3	14,800	16,300	14,200	10	–4	
11	1	21,400	29,800	24,900	39	16	
Average					50	42	–24
s.e.					12	12	9
Minimum					5	–4	–46
Maximum					200	187	50
Count					21	12	9

*Transients that did not lead to increased traction stress and were excluded from calculations. Traction stress (t.s.).

kdyne/cm^2 (~80% increase above baseline) about 30 seconds after the peak in calcium indicator fluorescence. The corresponding traction maps show an increase in the area of high traction stress (yellow to magenta) which begins at the lateral cell edges, and extends along the cell margin towards the front of the cell (Fig. 3A-C). Traction stress in these regions increases about tenfold, whereas only a 2-3-fold increase is seen within inner regions of the lamella. A band of increased traction stress also develops just in front of the cell body (Fig. 3B). Interestingly, this corresponds to the location where a high density of myosin II aggregates has previously been found in fish keratocytes (Svitkina et al., 1997). Approximately 35 seconds after the initial increase in $[Ca^{2+}]_i$ an abrupt retraction of the left lateral cell edge occurs (Fig. 3D,F), which is accompanied by a rapid drop in 90th percentile traction stress, to ~8 kdyne/cm^2 (~16% decrease from the peak value). During periods of increasing traction stress relatively little cell movement occurs (Fig. 3F, outlines B,C). However, following retraction cell speed increases together with a shortening of the cell's long axis (Fig. 3F, compare outline C with D). This is consistent with the previous suggestion that retraction at the rear releases cytoskeletal tension and allows cell movement to resume (Lee et al., 1999).

Although most calcium transients (21/23) are followed by an increase in traction stress production (Table 1), this is not always sufficient to induce retraction. When this occurs traction stress remains elevated even when $[Ca^{2+}]_i$ returns to baseline (Fig. 4C). Furthermore, in the absence of retraction, subsequent transients each lead to a step-wise increase in traction stress, until retraction is triggered (Fig. 4C). Thus multiple transients can have an additive effect on the increase in traction stress.

Our finding that virtually all calcium transients lead to an increase in traction stress, indicates that $[Ca^{2+}]_i$ acts to upregulate traction stress production. On average each transient leads to a 50% increase in traction stress, which ranges from 5-200% (Table 1). Conversely, since all retractions lead to rapid decreases in traction stress, they provide negative regulation of traction stress. Calcium transients that induce a retraction can result in an average decrease of ~12% below pre-transient, whereas there is no significant decrease in traction stress following transients that do not induce retraction (Fig. 4F).

The kinetic relationship between calcium transients and increases in traction stress

In many systems the cellular response is encoded in one or more features of the calcium signal, such as frequency, amplitude or duration (Berridge et al., 1997; Dolmetsch et al., 1997). Previously, we have observed that the frequency of calcium transients was higher in slow moving keratocytes compared with rapidly moving ones (Lee et al., 1999). Since

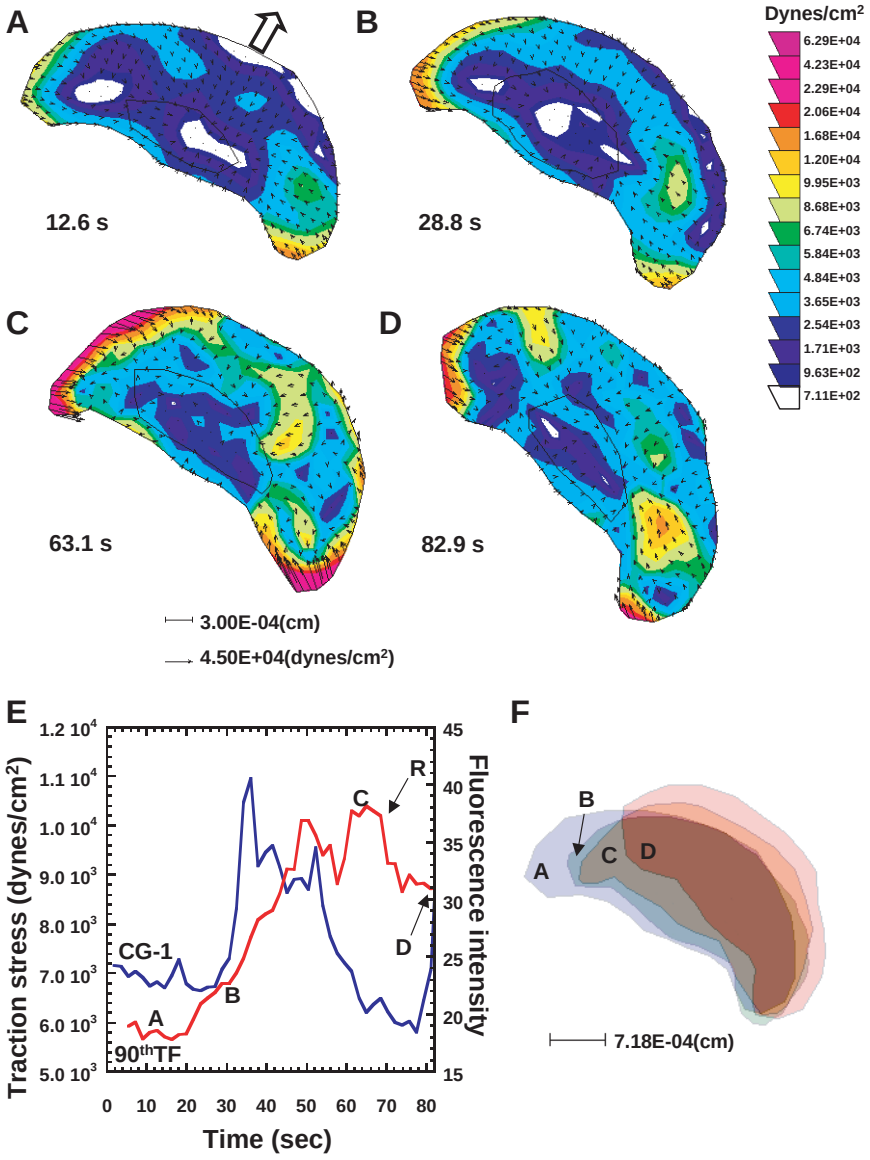

Fig. 3. The temporal relationship between calcium transients and increases in traction stress. Panels A-D are color-coded vector maps obtained at time points before (A), during (B) and after a calcium transient (C,D). (E) Plots of Calcium Green-1 fluorescence (CG-1) and values for the 90th percentile traction stress (TF 90) that were obtained from a running average of five data points. Following a calcium transient, an increase in traction stress occurs that is maintained following a decrease in $[Ca^{2+}]_i$ to baseline. Retraction (R) of the lateral rear edge results in a large decrease traction stress (D) yet this is elevated compared to pre-transient levels. (F) Cell outlines corresponding to the vector maps in panels A-D showing cell shape and movement with respect to the substratum.

these calcium transients form part of a mechano-chemical signaling mechanism, it is possible that some of their characteristics will influence traction force production.

To determine how transient elevations in $[Ca^{2+}]_i$ are coupled to increased in traction force production, the magnitude and duration of both the increases in calcium indicator fluorescence and traction stress were compared (Fig. 4). To aid comparison, examples calcium transients and subsequent changes in traction stress (Fig. 4A-C) are plotted on a relative scale. The magnitude and duration of both the calcium transients and increases in traction stress are variable (Table 2). However, there is a strong correlation between the duration of the calcium transient and both the magnitude (r=0.83) and duration (r=0.89) of the increase in traction stress. There is also a high degree of correlation between the magnitude of the calcium transient and the magnitude of the traction stress increase (r=0.76) but this is more weakly correlated with the duration of traction stress (r=0.65). Therefore, the form of the calcium transient has a strong influence on the kinetics of traction stress increase.

Another measure of the degree of coupling between the rise in $[Ca^{2+}]_i$ and the increase in traction stress is to compare the lag times between the initiation of a calcium transient and the onset of a rise in traction stress (Table 2). Although this is variable, an increase in traction stress is seen on average, 9 seconds following a calcium transient. However, most increases (18/21) in traction stress are seen within 20 seconds following the initial rise in $[Ca^{2+}]_i$. In some extreme cases (2/21), increases in traction stress can precede the initial rise in $[Ca^{2+}]_i$ by 5-15 seconds, or occur up to 40 seconds (1/21) afterwards. Since there can be some error in determining the start of a calcium transient, or rise in traction stress, the time interval between the peak values of calcium indicator fluorescence and traction stress was measured (Table 2). This was also variable, with an average peak to peak time interval of 23 seconds. However, the majority (17/21) of peak to peak intervals were less than 30 seconds. The delay times between a calcium transient and increased traction stress are consistent with the activation of downstream effectors of cytoskeletal

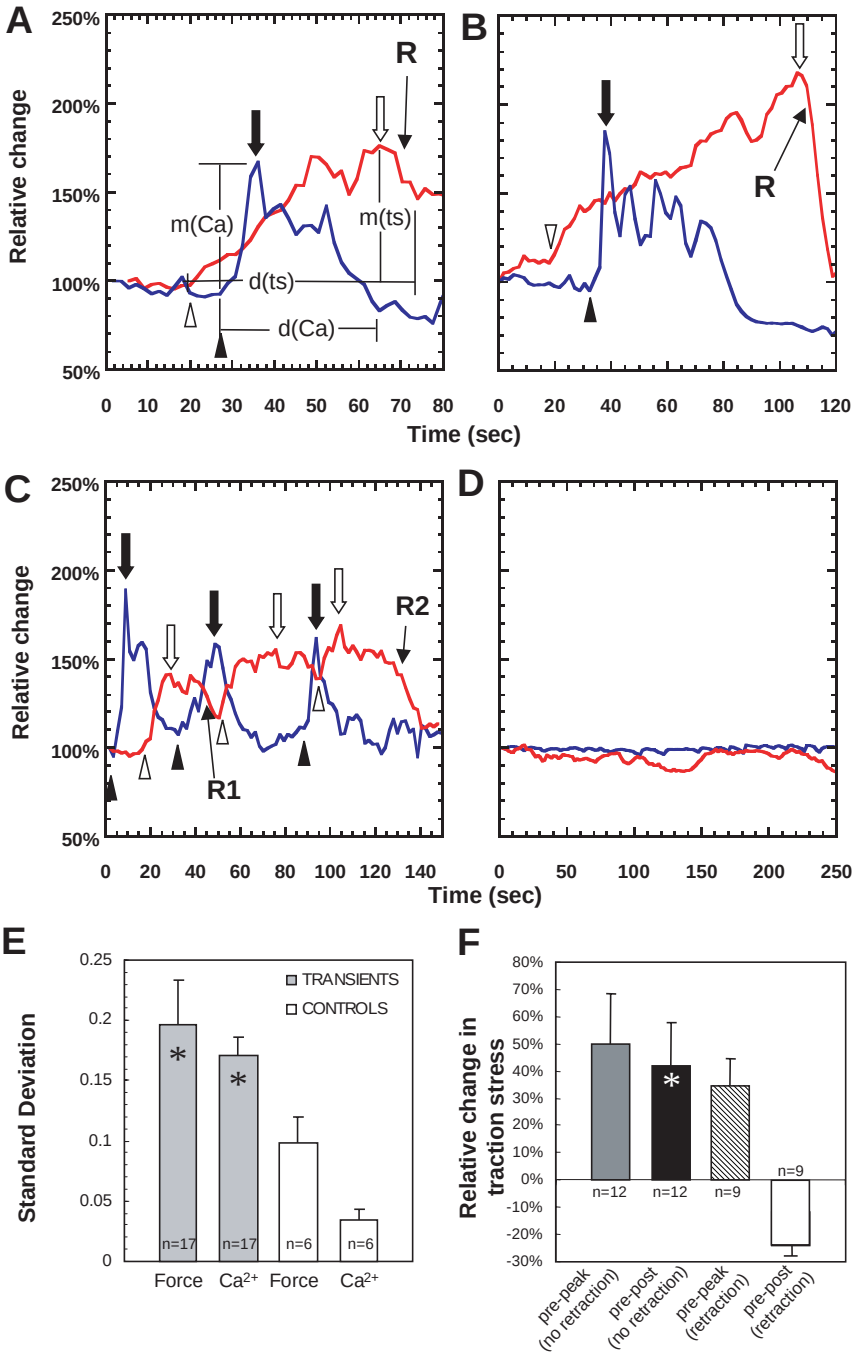

Fig. 4. The kinetic relationship between calcium transients and increases in traction stress in cells displaying calcium transients versus those that do not. Panels A-D are relative plots of Calcium Green-1 fluorescence and 90th percentile traction stress, where the first data point is set to 100% and retractions are indicated by R. Panel A is a relative plot of CG-1 fluorescence and traction stress from the transient shown in Fig. 3. Measurements of the increase in CG-1 fluorescence, m(Ca), and magnitude of traction stress, m(ts) are indicated by vertical lines. The duration of the calcium transient d(ts) and duration of increased traction stress, d(Ca) are indicated by horizontal lines. The initiation of a calcium transient and onset of increasing traction stress are indicated by closed and open arrowheads, respectively. The peak in CG-1 fluorescence and maximum traction stress are also indicated, respectively, by the closed and open arrows. Panel B is a relative plot of CG-1 fluorescence and traction stress from the transient shown in Fig. 5. Panel C shows an example of three calcium transients, each of which lead to a discrete increase in traction stress, such that a 'stepping-up' in traction stress occurs. Panel D shows a representative example of six cells in which no transients occur and subsequently no changes in traction stress are seen. Panel E shows a histogram of the average temporal fluctuation in traction stress in cells displaying transients (n=17) and in control cells that do not display transients (n=6). Temporal fluctuation of either CG-1 fluorescence or traction stress was obtained by normalizing the standard deviation of a measurement with respect to the mean of all measurements, for the entire period of observation, for each cell. Panel F shows the average percent increase in traction stress occurring from the pre-transient value (set to 0%) to the maximum value (peak) for transients where no retraction occurred (gray bar) and for transients followed by a retraction (shaded bar). The average percent decrease in traction stress occurring between pre-transient values to post-transient values, where no retraction occurred (black bar) and for transients followed by a retraction (open bar). Asterisks indicate statistically significant differences (P<0.05).

contractility, such as the activation of myosin light chain kinase by calcium-calmodulin (Siek et al., 2001). In addition these delay times are similar to the ~20 second interval observed in neutrophils between a calcium spike and retraction (Mandeville et al., 1995).

Temporal fluctuations in traction stress are dependent on calcium transients

Some keratocytes can move rapidly for 1-2 minutes without displaying calcium transients. It has been suggested this is because retraction is unimpeded and so cytoskeletal tension does not rise sufficiently to activate SACs. Nevertheless, it is possible that some small changes in traction stress may be occurring. To investigate, this we performed experiments in cells that did not display calcium transients for extended periods (40-60 seconds). Furthermore, we chose not to use calcium chelators or stretch activated ion channel blockers to inhibit transients, as these are likely to inhibit adhesion disassembly, which in turn may influence traction stress and cell motility. In all six cells examined negligible changes in traction stress occurred (Fig. 4D). To compare temporal fluctuations in traction stress between cells exhibiting calcium transients and those that do not (referred to here as control cells), the standard deviation of these fluctuations was normalized with respect to the average 90th percentile traction

Table 2. The kinetic relationship between calcium transients and increases in traction stress

Cell no.	Transient no.	B(Ca) – B(ts) (seconds)	P(Ca) – P(ts) (seconds)
1	1	3.60	7.20
	4	23.40	54.00
2	1	–5.43	30.05
	2	12.62	19.83
	2	21.03	25.24
	4	5.41	10.82
3	1	–16.20	72.00
	2	16.20	54.00
4	1	0.00	9.00
5	1	9.00	7.20
	2	1.80	43.20
	3	28.80	18.00
	4	12.60	21.60
6	1	4.15	6.86
7	1	2.05	4.17
8	1	8.41	17.58
9	1	0.00	0.03
10	2	40.25	27.65
	3	14.58	19.30
11	1	6.29	14.85
	2	–9.56	22.37
Average		9.04	23.09
s.e.		2.74	4.07
Minimum		–16.20	0.03
Maximum		40.25	72.00
Count		21.00	21.00

Beginning of calcium transient, B(Ca); beginning of increase in traction stress, B(ts); peak of calcium transient, P(Ca); maximum value of traction stress, P(ts)

stress for the entire period of observation, for each cell. The average normalized standard deviation was then obtained for changes in calcium indicator fluorescence and traction stress, for the group of cells displaying transients and control cells (Fig. 4E). It can be seen that the temporal fluctuations of calcium fluorescence and traction stress data in cells displaying transients, are both significantly greater than in control cells. These data confirm that calcium transients are involved in generating temporal fluctuations in traction stress and that these changes are associated with the SAC mediated feedback regulation of keratocyte movement.

A distinct change in spatial distribution of traction stress occurs during a calcium transient

To understand how calcium-induced increases in traction stress can trigger retraction that is specifically localized to the lateral rear margin, it is necessary to examine the change in spatial distribution of regions producing high traction stress. Since regions of high traction stress are sometimes observed at the leading edge, it is of interest to determine how this occurs without inducing retraction and loss of cell polarity.

In this example, the calcium transient leads to a large prolonged increase in traction stress, which decreases approximately 1 minute later (Fig. 5G). For this analysis, regions of highest traction stress are defined as those whose magnitude is equal or greater than the average 90th percentile (Fig. 5A-F, yellow to purple regions), for all traction maps in the series. Regions of highest traction stress begin to enlarge at the lateral cell edges and then expand along the cell margin, toward the front of the cell (Fig. 5A-F, Fig. 3A-C). As a result, traction stress at the leading edge increases approximately sevenfold. In some cases, regions of highest traction stress extend completely along the cell margin to include the front cell edge. Surprisingly, the magnitude of these traction stresses can equal that produced at the lateral rear margins, which may represent an approximately 30-fold increase in traction stress. When retraction occurs, the 90th percentile traction stress drops and regions of highest traction stress recede to the lateral rear edges (Fig. 5F, Fig. 3D). Thus these regions undergo cycles of enlargement and shrinkage, along the cell margin, during each calcium transient. This has been observed for all (21 out of 24) transients that lead to increases in traction stress. The consequence of these spatial changes in regions of highest traction stress is apparent when the change in area of these regions is ‘sampled’ within square regions, at set positions along the cell margin (Fig. 5F). It can be seen that regions of high traction stress at the lateral rear edges persist throughout the period of observation, and enlarge at about the same rate as the rise in 90th percentile traction stress (Fig. 5G,H). However, regions of highest traction stress at the front lateral edges and the leading edge exist for ~27 and ~17 seconds, respectively. In addition, these regions are relatively small and develop shortly before the peak in 90th percentile traction stress. We suggest that variations in the duration of highest traction stress, at different locations along the cell margin, have important implications for how they are utilized for cell movement.

Discussion

Using a new gelatin traction force assay in combination with calcium imaging, we have shown that single calcium transients induce a rapid increase in traction stress which is maintained or increases in a step wise manner, until retraction occurs. Thus calcium transients act as positive regulators of traction stress. Retraction of the cell margin is associated with an immediate drop in traction stress and so negatively regulates traction stress. In addition, we observe a distinct change in the spatial distribution of regions producing high traction stress. These regions begin to enlarge following a calcium-induced increase in traction stress and spread forwards along the cell margin. Surprisingly, regions of high traction stress can exist along the entire leading edge. Our findings suggest that calcium-induced changes in the magnitude and distribution of traction stress are important for maintaining the highly polarized organization of cytoskeletal function and is necessary for the rapid, highly directed, mode of keratocyte movement.

The increase in traction stress that follows elevations in $[Ca^{2+}]_i$ is not surprising, given the consensus regarding the role of calcium in contractile force generation in non-muscle cells (Katoh et al., 2001; Kamm and Stull, 2001). In addition the rise in traction stress that we observe prior to retraction, directly supports the role of calcium-dependent increases in cytoskeletal contractility in triggering detachment of the rear cell margin (Walker et al., 1998; Eddy et al., 2000; Qi Zeng et

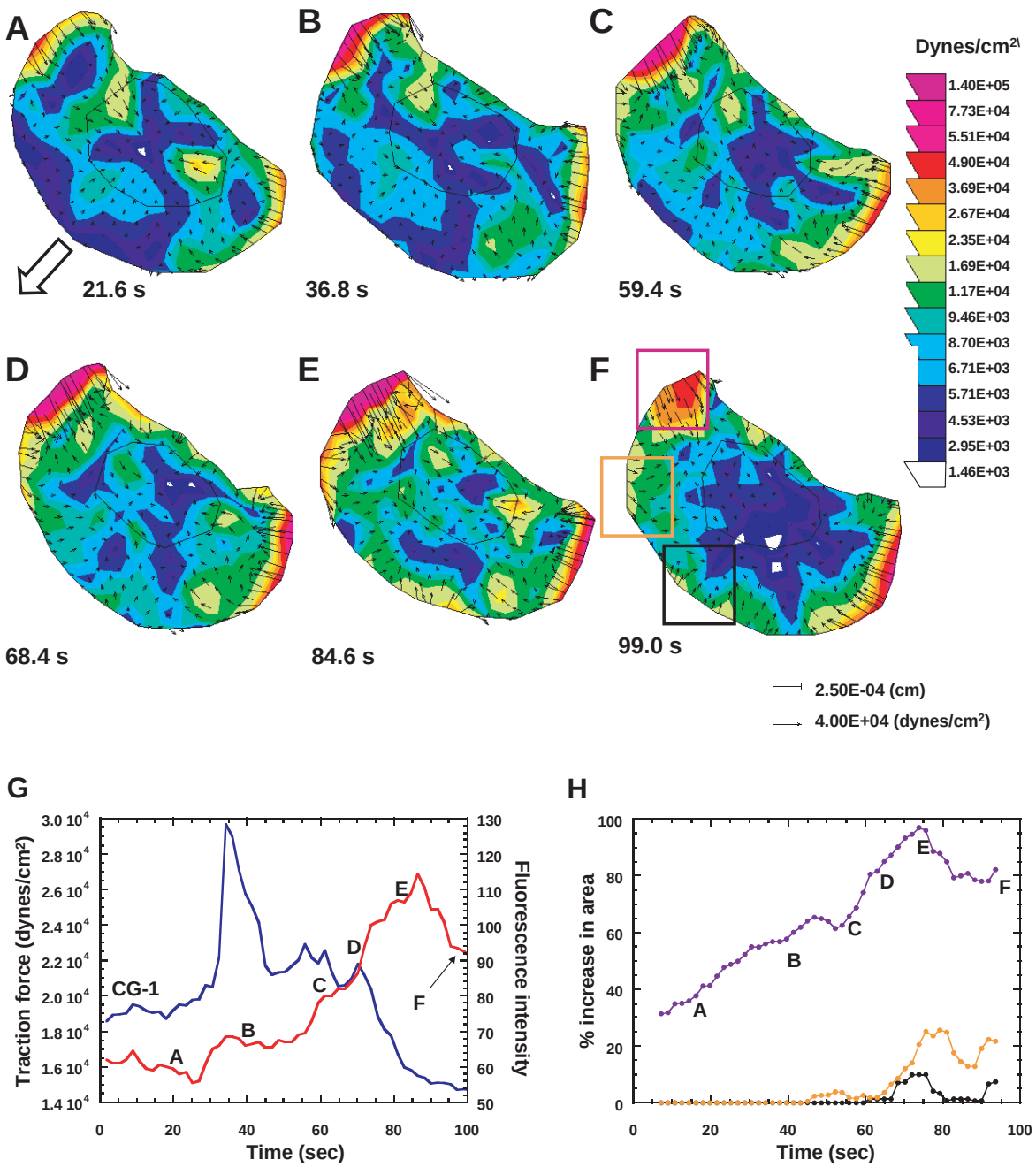

Fig. 5. Calcium transients induce distinct changes in the spatial organization of the highest traction stresses. Panels A-F are vector maps showing changes in distribution of the highest traction stresses (yellow-purple regions) during the calcium-induced rise in 90th percentile stress shown in panel G. Panel H shows the relative change in area of highest traction stresses within the square regions at the lateral rear edge (purple), the front lateral edge (yellow) and the leading edge (black) of the cell (panel F) moving in the direction indicated (bold arrow).

al., 2000). However, our finding that traction stress remains high for 10-15 seconds following the return of $[Ca^{2+}]_i$ to baseline, was unexpected since in other contractile systems force generation is reduced when $[Ca^{2+}]_i$ is lowered (Sieck et al., 2001). Therefore our results suggest that calcium transients act to positively regulate contractile force production, rather than providing both positive and negative regulation of contractility. One way in which a sustained increase in contractility could be accomplished is by sustaining the activity of MLCK after a calcium transient. It is therefore of interest that the activity of calmodulin-dependent kinase II (CaM kinase II) can be sustained by autophosphorylation, which 'traps' calmodulin causing the activity of both enzymes to be prolonged even when $[Ca^{2+}]_i$ returns to baseline (De Koninck and Schulman, 1998). Since MLCK is also a CaM kinase, it is possible that this represents a molecular mechanism by which an increased level of contractility could be maintained.

One advantage of this type of regulation is that it will promote detachment because the 'stepping-up' of contractile force will continue until it is sufficient to cause retraction. Thus

the degree of cytoskeletal contractility can be tuned to match the strength of cell-substratum adhesions. In other words, retraction will occur when contractile force exceeds a certain threshold for adhesion rupture, which we term an 'adhesion threshold'. This could account for the observation that multiple transients are required to trigger retraction in slow moving, fibroblastic-like keratocytes, whereas retraction can occur either without calcium transients or following only one transient, in rapidly moving keratocytes (Lee et al., 1999). Consistent with this, fibroblastic-like keratocytes appear to be more adhesive (Oliver et al., 1999) and so their adhesion threshold is likely to be higher than in rapidly moving cells.

The importance of adhesions in the generation and maintenance of traction stress is underscored by the precipitous drop in traction stress that we observe when retraction occurs. This is in accordance with previous observations of decreased 'wrinkling' of flexible silicone substrata following retraction (Lee et al., 1999). Therefore, calcium-induced cell detachment is the major negative regulator of traction stress and is consistent with the proposal that SAC activation leads to a reduction in cytoskeletal tension by inducing retraction (Lee et al., 1999). Cell-substratum adhesions may also contribute to calcium-induced elevations in traction stress, by strengthening in response to increased contractile force. Support for this comes from observations of increased traction force production when cytoskeletal contractility and focal adhesion formation increase concomitantly (Chrzanowska-Wodnicka and Burridge, 1996; Burridge and Chrzanowska-Wodnicka, 1996; Roy et al., 1999). It is also possible that increased $[Ca^{2+}]_i$ affects adhesion strength directly by enhancing integrin-mediated adhesion (Pelletier et al., 1992; Sjaastad et al., 1994; Sjaastad and Nelson, 1996).

The response of adhesions to cytoskeletal tension could explain the change in spatial distribution of high traction stress, that we observe following a calcium transient. A striking feature of this change, is that regions of high traction stress propagate toward the front of the cell, within a narrow region along the cell margin. Interestingly, this corresponds to the location of a band of very close cell-substratum adhesions in keratocytes (Lee and Jacobson, 1997). Since this region is in more intimate contact with the substratum than elsewhere, the forward propagation of increased traction stress should occur preferentially along the lateral cell edges and could also involve a coordinated sequence of adhesion strengthening. Furthermore, the direction in which regions of high stress enlarge, seems to reflect the efficacy with which different regions of the cytoskeleton can contract. Thus the initial increase in traction stress at the lateral rear margins could reflect the more rapid and extensive contraction of stress fibers in this region (Katoh et al., 2001) while the actin meshwork within the lamella contracts more slowly. This agrees with the relatively sparse distribution of myosin II minifilaments toward the front of the lamella, compared with the rear (Svitkina et al., 1997).

We propose that the spatio-temporal changes in traction stress that we observe following a SAC calcium transient, act to maintain the highly polarized distribution of cytoskeletal function that is required for rapid movement (Fig. 6). Thus regions of high traction stress are usually localized to the lateral cell edges, to facilitate retraction, while very small or undetectable tractions exist at the leading edge, to promote protrusion simultaneously (Fig. 6, stage 1). When SAC activation triggers a calcium transient (Fig. 6, stage 2) regions of highest traction stress at the cell rear begin to enlarge. The continuation of this process results in long periods of increased traction stress at the lateral rear cell edges (Fig. 6, stages 2-5). This could promote retraction by 'priming' adhesion complexes for disassembly as has been suggested for fibroblasts (Burridge et al., 1996) by acting cooperatively with calcium-dependent adhesion disassembly mechanisms (Crowley and Horwitz, 1995). In contrast, brief, infrequent periods of high traction stress at the leading edge (Fig. 6, stage 5) could be sufficient to provide occasional bursts of propulsive traction while being too short to induce retraction. In relation to this, the activity of Rac has recently been found to be regulated by the direction of mechanical stress applied to the cell edge (Katsumi et al., 2002). Increased tangential stress inhibited Rac activity, while stress applied inward and perpendicular to the edge relieved this inhibition. Therefore, it is possible that brief increases in inward-directed traction stress at the leading edge promote the activity of Rac, and thus the rate of protrusion. Regions of increased traction stress at the front lateral edges are intermediate in duration compared with either the front or rear cell margins (Fig. 6, stage 4). Interestingly, it is in these regions that focal adhesion-like structures (Lee and Jacobson, 1997) and new stress fibers are first seen to appear (Svitkina et al., 1997). Therefore, we suggest that increased contractility at the lateral front edge of the cell may be primarily involved in inducing the formation of new load bearing cytoskeletal structures to replace those that are being lost at the rear during retraction. In turn this allows a region of high cytoskeletal tension to be maintained perpendicular to the direction of cell movement, which is

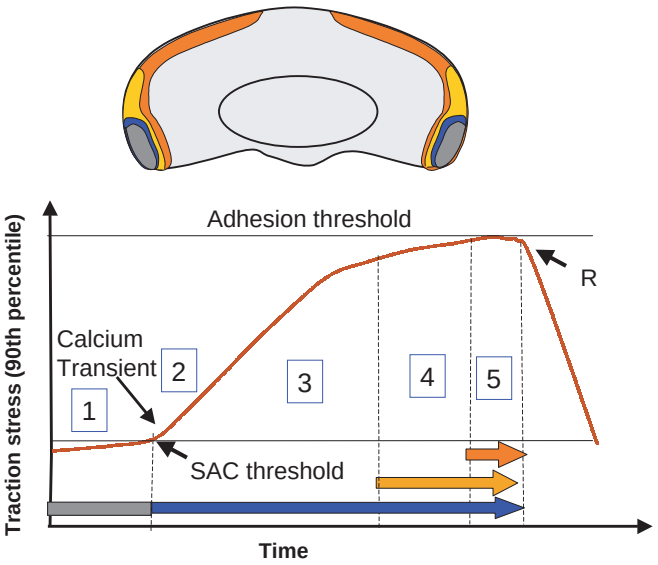

Fig. 6. Diagram illustrating the changes in size and spatial distribution of regions producing the highest traction stress. Colored zones within the keratocyte represent the temporal sequence (blue, yellow, red) in which regions of highest traction stress enlarge, following a calcium transient. The graph shows the duration of each region, with respect to the increase in 90th percentile traction stress (red line), represented by the length of matching colored arrows. The numbered boxes represent different stages of the mechano-chemical feedback cycle as explained in the text.

important for the rapid highly directed mode of keratocyte locomotion (J.L., unpublished).

Our results suggest that the mechano-sensory response of cell-substratum adhesions provides local feedback regulation of traction stress in response to global changes in cytoskeletal contractility. In turn, this provides insight into how the spatial pattern of traction stresses is inextricably linked to cell shape and mode of movement. Further studies into how adhesions respond to force, and the effect this has on lamellar dynamics, will be important for understanding how mechano-sensing via cell-substratum adhesions and SACs are coordinated with each other.

We thank Micah Dembo for his critique of this manuscript and suggestions regarding data analysis. This work was supported by a National Science Foundation Grant MCB-0114231 to J.L.

References

Balaban, N. Q., Schwarz, U. S., Riveline, D., Goichberg, P., Tzur, G., Sabanay, I., Mahalu, D., Safran, S., Bershadsky, A and Addadi, L. (2001). Force and focal adhesion assembly: a close relationship studied using elastic micropatterned substrates. *Nat. Cell Biol.* **3**, 466-472.

Berridge, M. J. (1997). The AM and FM of calcium signalling. *Nature* **386**, 759-760.

Brundage, R. A., Fogarty, K. E., Tuft, R. A. and Fay, F. S. (1991). Calcium gradients underlying polarization and chemotaxis of eosinophils. *Science* **254**, 703-706.

Burridge, K. and Chrzanowska-Wodnicka, M. (1996). Focal adhesions, contractility, and signaling. *Annu. Rev. Cell Dev. Biol.* **12**, 463-518.

Burton, K., Park, J. H. and Taylor, D. L. (1999). Keratocytes generate traction forces in two phases. *Mol. Biol. Cell* **10**, 3745-3769.

Cheek, T. (1989). Spatial aspects of calcium signalling. *J. Cell Sci.* **93**, 211-216.

Chew, T. L., Wolf, W. A., Gallagher, P. J., Matsumura, F. and Chisholm, R. L. (2002). A fluorescent resonant energy transfer-based biosensor reveals transient and regional myosin light chain kinase activation in lamella and cleavage furrows. *J. Cell Biol.* **156**, 543-553.

Choquet, D., Felsenfeld, D. P. and Sheetz, M. P. (1997). Extracellular matrix rigidity causes strengthening of integrin-cytoskeleton linkages. *Cell* **88**, 39-48.

Chrzanowska-Wodnicka, M. and Burridge, K. (1996). Rho-stimulated contractility drives the formation of stress fibers and focal adhesions. *J. Cell Biol.* **133**, 1403-1415.

Citi, S. and Kendrick-Jones, J. (1987). Regulation of non-muscle myosin structure and function. *BioEssays* **7**, 155-159.

Crowley, E. and Horwitz, A. F. (1995). Tyrosine phosphorylation and cytoskeletal tension regulate the release of fibroblast adhesions. *J. Cell Biol.* **131**, 525-537.

De Koninck, P. and Schulman, H. (1998). Sensitivity of CaM kinase II to the frequency of Ca2+ oscillations. *Science* **279**, 227-230.

Dembo, M. and Wang, Y.-L. (1999). Stresses at the cell-to-substrate interface during locomotion of fibroblasts. *Biophysical J.* **76**, 2307-2316.

Dolmetsch, R. E., Lewis, R. S., Goodnow, C. C. and Healy, J. I. (1997). Differential activation of transcription factors induced by Ca2+ response. *Nature* **386**, 855-760.

Doyle, A. D. and Lee, J. (2002). Simultaneous, real-time imaging of intracellular calcium and cellular traction force production. *Biotechniques* **33**, 358-364.

Eddy, R., Pierini, L. M., Matsumura, F. and Maxfield, F. R. (2000). Ca2+-dependent myosin II activation is required for uropod retraction during neutrophil migration. *J. Cell Sci.* **113**, 1287-1298.

Galbraith, C. G. and Sheetz, M. P. (1997a). A micromachined device provides a new bend on fibroblast traction forces. *Proc. Natl. Acad. Sci. USA* **94**, 9114-9118.

Galbraith, C. G. and Sheetz, M. P. (1997b). Relationship between cell shape, traction force and speed. *Mol. Biol. Cell Suppl.* **8**, 385.

Giannone, G., Ronde, P., Gaire, M., Haich, J. and Takeda, K. (2002). Calcium oscillations trigger focal adhesion disassembly in human U87 astrocytoma cells. *J. Biol. Chem.* **277**, 26364-26371.

Gilbert, S. H., Perry, K. and Fay, F. S. (1994). Mediation of chemoattractant-induced changes in [Ca2+]i and cell shape, polarity and locomotion by InsP3, DAG, and protein kinase C in newt eosinophils. *J. Cell Biol.* **127**, 489-503.

Glogauer, M., Arora, P., Yao, G., Sokholov, I., Ferrier, J. and McCulloch, C. A. G. (1997). Calcium ions and tyrosine phosphorylation interact coordinately with actin to regulate cytoprotective responses to stretching. *J. Cell Sci.* **110**, 11-21.

Goekeler, Z. M. and Wysolmerski, R. B. (1995). Myosin light chain kinase regulated endothelial cell contraction:the relationship between isometric tension, actin polymerization and myosin phosphorylation. *J. Cell Biol.* **130**, 613-627.

Hartwig, J. H. and Yin, H. (1988). The organization and regulation of the macrophage cytoskeleton. *Cell Motil. Cytoskeleton* **10**, 117-125.

Hendey, B., Klee, C. B. and Maxfield, F. R. (1992). Inhibition of neutrophil chemokinesis on vitronectin by inhibitors of calcineurin. *Science* **258**, 296-299.

Huttenlocher, A., Palecek, S. P., Lu, Q., Zhang, W., Mellgren, R. L., Lauffenburger, D. A., Ginsberg, M. H. and Horwitz, A. F. (1997). Regulation of cell migration by the calcium-dependent protease calpain. *J. Biol. Chem.* **272**, 32719-32722.

Ishihara, A., Gee, K., Schwartz, S., Jacobson, K. and Lee, J. (1997). Photoactivation of caged compounds in single, living cells: An application to the study of cell locomotion. *Biotechniques* **23**, 268-274.

Kamm, K. E. and Stull, J. T. (2000). Dedicated myosin light chain kinases with diverse cellular functions. *J. Biol. Chem.* **276**, 4527-4530.

Katoh, K., Kaibuchi, Y. and Fujiwara, K. (2001). Rho-kinase-mediated contraction of isolated stress fibers. *J. Cell Biol.* **153**, 569-583.

Katsumi, A., Milanini, J., Kiosses, W. B., del Pozo, M. A., Kaunas, R., Chien, S., Hahn, K. M. and Scwartz, M. A. (2002). Effects of cell tension on the small GTPase Rac. *J. Cell Biol.* **158**, 153-164.

Kolega, J. (1986). Effects of mechanical tension on protrusive activity and microfilament and intermediate filament organization in an epidermal epithelium moving in culture. *J. Cell Biol.* **102**, 1400-1411.

Lauffenburger, D. A. and Horwitz, A. F. (1996). Cell migration: a physically integrated molecular process. *Cell* **84**, 359-369.

Lee, J., Ishihara, A., Oxford, G., Johnson, B. and Jacobson, K. (1999). Regulation of cell movement is mediated by stretch-activated calcium channels. *Nature* **400**, 382-386.

Lee, J., Ishihara, A., Theriot, J. and Jacobson, K. (1993). Principles of locomotion for simple-shaped cells. *Nature* **362**, 167-171.

Lee, J. and Jacobson, K. (1997). The composition and dynamics of cell-substratum adhesions in locomoting fish keratocytes. *J. Cell Sci.* **110**, 2833-2844.

Lee, J., Leonard, M., Oliver, T., Ishihara, A. and Jacobson, K. (1994). Traction forces generated by locomoting keratocytes. *J. Cell Biol.* **127**, 1957-1964.

Lo, C.-M., Wang, H.-B., Dembo, M. and Wang, Y.-L. (2000). Cell movement is guided by the rigidity of the substrate. *Biophys. J.* **79**, 144-152.

Mandeville, J. T., Ghosh, R. N. and Maxfield, F. R. (1995). Intracellular calcium levels correlate with speed and persistent forward motion in migrating neutrophils. *Biophys. J.* **68**, 1207-1217.

Marganski, W. A., Dembo, M. and Wang, Y.-L. (2003). Measurements of cell-generated deformations on flexible substrata using correlation-based optical flow. *Methods Enzymol.* **161**, 197-211.

Marks, P. W. and Maxfield, F. R. (1990). Transient increases in cytosolic free calcium appear to be required for the migration of adherent human neutrophils. *J. Cell Biol.* **110**, 43-52.

Mitchison, T. J. and Cramer, L. P. (1996). Actin-based cell motility and cell locomotion. *Cell* **84**, 371-379.

Munevar, S., Wang, Y.-L. and Dembo, M. (2001). Traction force microscopy of normal and H-ras transformed 3T3 fibroblasts. *Biophys. J.* **80**, 1744-1757.

Nebl, T. and Fisher, P. R. (1997). Intracellular Ca2+ signals in Dictyostelium chemotaxis are mediated exclusively by Ca2+ influx. *J. Cell Sci.* **110**, 2845-2853.

Oliver, T., Dembo, M. and Jacobson, K. (1999). Separation of propulsive and adhesive traction stresses in locomoting keratocytes. *J. Cell Biol.* **145**, 589-604.

Palecek, S. P., Huttenlocher, A., Horwitz, A. F. and Lauffenburger, D. A. (1998). Physical and biochemical regulation of integrin release during rear detachment of migrating cells. *J. Cell Sci.* **111**, 929-940.

Pelletier, A. J., Bodary, S. C. and Levinson, A. D. (1992). Signal transduction by the platelet integrin alpha IIb beta 3: induction of calcium oscillations required for protein-tyrosine phosphorylation and ligand-induced spreading of stably transfected cells. *Mol. Biol. Cell* **3**, 989-998.

Pollard, T. D. and Borisy, G. G. (2003). Cellular motility driven by assembly and disassembly of actin filaments. *Cell* **112**, 453-465.

Rees, D. A., Charlton, J., Ataliotis, P., Woods, A., Stones, A. J. and Bayley, S. A. (1989). Myosin regulation and calcium transients in fibroblast shape change, attachment and patching. *Cell Motil. Cytoskeleton* **13**, 112-122.

Riveline, D., Zamir, E., Balaban, N. Q., Schwarz, U. S., Ishizaki, T., Narumiya, S., Kam, Z., Geiger, B. and Bershadsky, A. (2001). Focal contacts as mechanosensors: Externally applied local mechanical force induces growth of focal contacts by an mDia-dependent and ROCK-independent mechanism. *J. Cell Biol.* **153**, 1175-1185.

Roy, P., Petroll, W. M., Cavanagh, H. D. and Jester, J. V. (1999). Exertion of tractional force requires the coordinated up-regulation of cell contractility and adhesion. *Cell Motil. Cytoskeleton* **43**, 23-43.

Sieck, G. C., Han, Y.-S., Pabelick, C. M. and Prakask, Y. S. (2001). Temporal aspects of excitation-contraction coupling in airway smooth muscle. *J. Appl. Physiol.* **91**, 2266-2274.

Sjaastad, M., Angres, B., Lewis, R. S. and Nelson, J. (1994). Feedback regulation of cell-substratum adhesion by integrin-mediated intracellular Ca2+ signaling. *Proc. Natl. Acad. Sci. USA* **91**, 8214-8218.

Sjaastad, M. D. and Nelson, J. (1996). Integrin-mediated calcium signaling and regulation of cell adhesion by intracellular calcium. *Bioassays* **19**, 47-55.

Svitkina, T. M., Verkhovsky, A. B., Quade, K. M. M. and Borisy, G. C. (1997). Analysis of the actin-myosin II system in fish epidermal keratocytes: mechanism of cell body translocation. *J. Cell Biol.* **139**, 397-415.

Tan, J. L., Tien, J., Pirone, D. M., Gray, D. S., Bhadriraju, K. and Chen, C. S. (2003). Cells lying on a bed of microneedles: an approach to isolate mechanical force. *Proc. Natl. Acad. Sci. USA* **100**, 1484-1489.

Walker, J. W., Gilbert, S. H., Drummond, R. M., Yamada, M., Sreekumar, R., Carraway, R. E., Ikeebe, M. and Fay, F. (1998). Signaling pathways underlying eosinophil cell motility revealed by using caged peptides. *Proc. Natl. Acad. Sci. USA* **95**, 1568-1573.

Wang, Y.-L. and Pelham, R. J. (1998). Preparation of a flexible porous polyacrylamide substrate for mechanical studies of cultured cells. *Methods Enzymol.* **298**, 489-496.

Zeng, Q., Lagunoff, D., Masaracchia, R., Goeckeler, Z. and Cote, G. (2000). Endothelial cell retraction is induced by PAK2 monophosphorylation of myosin II. *J. Cell Sci.* **113**, 471-482.